Received: 20 August 2023 | Revised: 5 December 2023 | Accepted: 9 January 2024

IET Renewable Power Generation

DOI: 10.1049/rpg2.12939

The Institution of Engineering and Technology WILEY

ORIGINAL RESEARCH

Voltage dip propagation in renewable-rich power systems utilizing grid-forming converters

Rafat Aljarrah[1] | **Mazaher Karimi**[2] | **Rasoul Azizipanah-Abarghooee**[3] | **Qusay Salem**[1] | **Sahban Alnaser**[4]

[1]Electrical Engineering Department, Princess Sumaya University for Technology, Amman, Jordan

[2]School of Technology and Innovations, University of Vaasa, Vaasa, Finland

[3]Energy Advisory Department, WPS, Manchester, UK

[4]Electrical Engineering Department, The University of Jordan, Amman, Jordan

Correspondence
Mazaher Karimi, School of Technology and Innovations, University of Vaasa, 65200, Vaasa, Finland.
Email: mazaher.karimi@uwasa.fi

Funding information
University of Vaasa, Grant/Award Number: CIRP-5G; Business Finland, Grant/Award Number: 6937/31/2021

Abstract

The growing integration of converter-interfaced renewable energy sources (RESs) utilizing Grid-Following (GFL) converters has displaced conventional synchronous generators (SGs) in central generation units. This shift presents challenges, including diminished system inertia, lower fault levels, and implications for system strength and network resilience. The propagation of voltage dips, particularly during disturbances like system Short Circuit (SC) faults, is adversely affected by the increased penetration of such RESs. This is attributed to the limited support capability of these sources and their distinct SC response compared to SGs. In response to these challenges, Grid-Forming (GFM) converters emerge as a promising technology equipped with advanced functionalities that emulate SG operation. Consequently, they hold potential for mitigating the effects of voltage dip propagation in renewable-rich power systems. This study aims to assess the impact of employing GFM converters in renewable-rich power systems on voltage dip propagation across the network. The authors' investigation begins by examining the SC response of GFM converters and comparing it with the responses of traditional GFL converters and SGs. The paper proceeds to analyze voltage dip propagation, considering various penetration scenarios involving RESs based on GFL and GFM converters. The IEEE 9-BUS test system, implemented in the DIgSILENT PowerFactory software, serves as the basis for these evaluations. Through extensive simulations and analysis, the authors' research provides valuable insights into the effectiveness of GFM converters in enhancing the network's response to voltage dips.

1 | INTRODUCTION

Increasing the penetration of converter-interfaced Renewable Energy Sources (RESs) such as wind and photovoltaic (PV) is a goal for many grid operators and policy makes worldwide. Such increased penetration is accompanied with decommissioning of large Synchronous Generators (SGs) which have been traditionally the source for system inertia and system strength [1, 2]. As a result of reducing the amount of online SGs in the systems, the system inertia and the fault level would be reduced; hence, system strength is going to be reduced too [2]. It is worth noting that the fault level might fail to accurately reflect the system strength in scenarios of high penetration of converter-based RESs. However, it can still be used, to an extent, as an indicator of the system strength regarding the voltage sensitivity to the penetration level of such RESs. In this context, the reduced system strength would lead to operating more weaker grids due to the limited capability of the currently utilized Grid-Following (GFL) converters in supporting the grid when compared to the original classical systems [3]. Consequently, power systems with high penetration of RESs might suffer from severe problems. One of the main issues might be raised because the system strength deterioration is the voltage dip propagation through wider scale areas in the network when exposed to disturbances, for example, Short Circuit (SC) faults [4]. This is due to the direct relationship which exists between the system strength and the resulting voltage deviation in case of disturbance incidents. For instance, as the fault levels decrease, the voltage step

increases proportionally. Hence, the increased penetration of RESs when accompanied with decommissioning of large SG units would lead to reducing the dynamic voltage support available in the grid which is an essential in order to limit the voltage dip propagation, and to achieve a smooth voltage recovery after clearing the faults, hence, avoiding voltage collapse [5–7].

The currently utilized converters technology are considered GFL converters as they follow the grid voltage and phase, and they rely on the stability and the strength of the grid to function properly. Although GFL converters are required to support the grid voltage and to ride through the fault during disturbances, the stable operation of such GFL converters assumes that inertial sources (e.g. SGs) would regulate the system stability and would ensure the minimum requirement of system strength. This might be valid to an extent in low RESs penetration scenarios but not in future low inertia scenarios where most of the power demand would be met by RESs [8]. Although traditional GFL-based RESs have been usually controlled in such a way to provide dynamic voltage support by injecting more reactive power during faulty conditions, the response of the converter is limited to the capped overrating capability which cannot exceed a certain level around the ratings of the device. Moreover, the speed of the response and the injected reactive current might be delayed due to the measurements, the communication and the other factors which might negatively affect their fault contribution and the voltage level during and after the faulty conditions.

Consequently, the voltage support task during the faults is going to deteriorate in high penetration scenarios of GFL-based RESs and therefore enhanced technologies or other mitigating solutions might be essentially required to avoid wide scale voltage dip propagation through the networks [9, 10]. In this regard, Grid-Forming (GFM) converters have been recently proposed as a promising substitution for the lack of functionalities that SGs have traditionally provided as an alternative for GFL converters that fail to do so [8, 11]. Such converters, which act as a controllable voltage source and produce voltage and frequency in the system, are a dependable substitute for grid following converters [11]. In the grid-forming mode, the converter is robustly synchronized to the grid, and in the event of any disruption, the issue is immediately resolved without the need for a phase-locked loop (PLL). Hence, in contrast to conventional GFL converters, GFM converters have special properties which enable them to deliver a steadily stable voltage and frequency output to the grid, even in situations where a grid connection is not available. In other words, they are capable of actively regulating and adjusting the voltage and frequency aspects independently from the grid. Hence, they are forming the grid [12].

According to [13, 14], in comparison to GFL converters, these GFM converters have a better dynamic behaviour in terms of voltage stability. In addition, GFM converters consist of a group of voltage-controlled converters that actively preserve the internal voltage phasor throughout the sub-transient and transient time intervals [15]. GFM converters can be categorized based on the control strategies into three types: Droop-based control, virtual synchronous machines, and virtual oscillator controllers [12]. A part of the advantageous properties of the grid-forming converters is improving the system stability and supporting the grid inertia. It is expected that GFM converters would contribute to mitigating the severity of the voltage dip propagation through the network when utilized instead of GFL ones traditionally utilized to interface RESs. It is worth pointing that this issue has not investigated well in the up-to-date literature. Hence, this paper intends to contribute to this regard by examining the suitability of employing GFM converters in mitigating the impact of the severity of voltage dip propagation in renewable-rich power systems. For this reason, the Droop-based GFM converters are picked for this examination in this study as an example of GFM converters technologies that are widely suggested in the literature.

The rest of the paper is organized as follows: Section 2 presents an overview of voltage dip propagation power systems with a focus on the impact of increased penetration of RESs. Section 3 introduces the concept of modelling and control of droop-based GFM converters. Section 4 presents the methodology of the research. Section 5 analyses and discusses the results. And finally, Section 6 concludes the paper.

2 | CONTROL OF DROOP-BASED GFM CONVERTERS

This section aims to shed a light on the droop-based GFM converters modelling and control despite that the target of the paper is not to optimize the control behaviour. Droop-based GFM converters frequently employ the droop control technique, which enables them to adjust the output frequency and voltage responding to variations in grid conditions. Thanks to this droop-based control method, the converter can operate with a flexible output characteristic, which helps effective power sharing with other connected sources and helps maintain grid stability [13, 16].

In addition, the converter can quickly adjust to changes in load demand or variations in grid parameters by using droop control while maintaining stable voltage and frequency outputs. In other words, it contributes to balancing the load and the generation in the network. Unlike the GFL converters, Droop-based GFM converters do not rely on tracking the real and reactive power references, instead the active and reactive power output are adjusted in response to variations of voltage and frequency monitored at the terminals of the converters [17]. The overall objective control target enables voltage source behaviour of the converter that is equipped with inertia in the voltage angle to overcome the issues raised when considering fast current control loops in the GFL converters.

In this work we have adopted the droop-based GFM model reported in [16] which is available in DIgSILENT PowerFactory for root mean square (RMS) and electromagnetic transient (EMT) simulations. The layout structure of the droop-based GFM model is shown in Figure 1. It can be noticed that the inductor-capacitor-inductor (LCL)-filter is integrated with the inverter and its control frame. It is worth noting that a virtual impedance is also implemented with the converter to improve

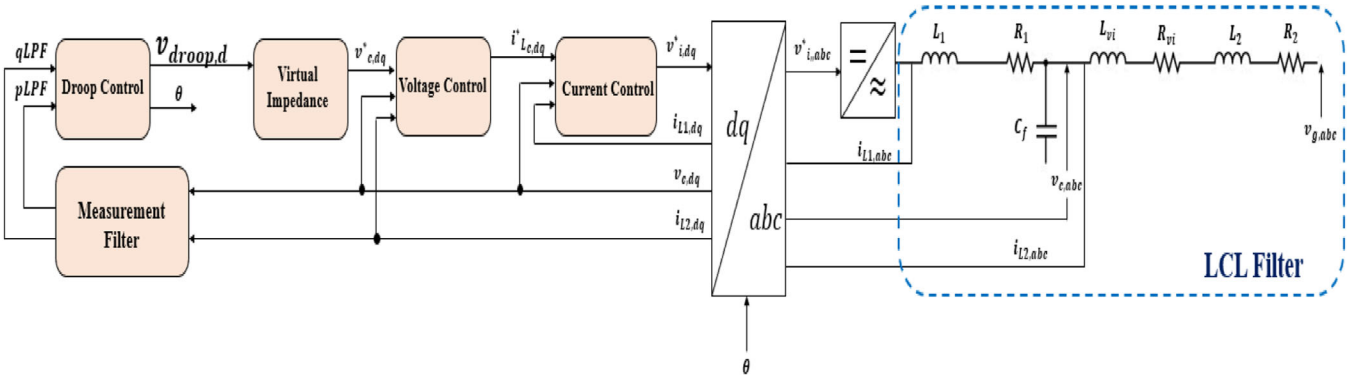

FIGURE 1 Layout of droop-based GFM converter [16]. GFM, grid-forming.

the damping and provide current limiting task in the event of SC faults [16, 18]. Hence, the existence of such impedance would affect the SC characteristics of the GFM converter and limit its current contribution to a certain level. Both the frequency droop $\boldsymbol{\omega_{droop}}$, and voltage droop $\boldsymbol{v_{droop}}$, are calculated using the measured and filtered values of active ($\boldsymbol{p_{LPF}}$) and reactive ($\boldsymbol{q_{LPF}}$) power, according to the droop coefficients ($\boldsymbol{m_\omega}$ and $\boldsymbol{m_v}$), shown in (1) and (2) [16].

$$\omega_{droop} = \omega_0 + m_\omega \left(p_{LPF} - p_0\right) \tag{1}$$

$$v_{droop,d} = v_0 + m_v \left(q_{LPF} - q_0\right) \tag{2}$$

where $\boldsymbol{\omega_0}$ and $\boldsymbol{v_0}$ are set to 1 p.u., while $\boldsymbol{p_0}$ and $\boldsymbol{q_0}$ are set to zero. The integration of $\boldsymbol{\omega_{droop}}$ is used for the angle of the park transformation.

It is worth noting that the cascaded voltage and current controllers and the physical model of the converter are implemented in the d-q frame considering balanced conditions. The inner voltage and current controllers are almost similar as they consist of PI-controllers for each axis, the decoupling and the feed-forward of the output current with feedforward gain. Although they both might be modelled and considered, their dynamics may be simplified or neglected as the inner control loops have time constants that are significantly smaller time constants when compared with the droop control measurements filter [16]. Hence, in this model, which is implemented in DIgSILENT PowerFactory, the controller of the GFM converter does not contain inner current control loop while the voltage control loop is considered. Note that the current limitation functions are implemented in a separate output voltage block based on the voltage drop through the virtual impedance and no further current limitations are considered in the inner current control loop [19].

3 | METHODOLOGY

The research methodology in this work would first include investigating the SC behaviour of the utilized GFM converter in comparison to the traditional GFL converter during SC faults. Then, it examines the voltage dip propagation during SC faults in SGs-based systems without including RESs. This is aimed at providing the base scenario for later comparison with the other scenarios where RESs are considered instead of the SGs. After that, the analysis would cover creating several RESs penetration scenarios that are equipped with the traditional GFL converter interfaces (More specifically, high penetration scenarios of type-4 wind generation) to examine the voltage dip propagation after exposing the system to disturbances such as three-phase bolted SC faults. The sensitivity of the voltage dip propagation to the increased RESs penetration will be tested and analysed. Finally, the GFM converters would be introduced to replace the GFL converters to examine the impact of the advanced supporting functionalities of the introduced GFM converters on the propagation of the voltage dip considering the same studied scenarios.

Results of both cases of GFL and GFM converters utilized for interfacing RESs would be compared and analysed considering the different studied scenarios of RESs' penetration. It is worth noting that those droop-based GFM converters described above, available in DIgSILENT PowerFactory, are only examined here, while the other types of GFM technologies, namely virtual synchronous machines, and virtual oscillator controllers, are beyond the aim of this research.

4 | RESULTS AND DISCUSSIONS

4.1 | Short-circuit current contribution from GFL and GFM converters

To better understand the different behaviour of both the GFL and GFM converters in terms of their dynamic support during voltage dip events, the SC circuit behaviour is analysed. For this purpose, a simple-test system is built that consists of a 11-kV grid, 0.4/11 kV step up transformer that connects the converters to the grid, as shown in Figure 2. A symmetrical bolted three-phase SC fault has been initiated and both the GFL and GFM converters are tested one a time. The SC current contribution is captured for comparison purposes as shown in Figure 3. It is worth pointing that the maximum current injection during

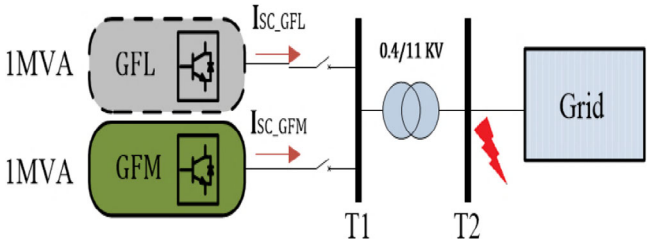

FIGURE 2 Test system for SC current contribution. SC, short circuit.

the SC event is typically limited to a pre-defined value of around the rated of the converters (e.g. 1–1.5 p.u.) to protect the switches of the converter interface [20, 21]. This work sets these maximum currents to 1.2 p.u. for both converters. Observe the fault contribution of the GFL converter shown in Figure 3a, where the SC current is decomposed to a very short transient that decays in the first cycle. It can be observed that this transient might reach different values according to different phases. The maximum transient shown in Figure 3a has reached 1.6 p. u, in phase c. In addition to the transient current, the GFL converter shows a steady-state fixed value that is limited to the maximum overrating capability of the converter (i.e. 1.2 p.u.).

On the other hand, the fault contribution of GFM converter has shown a distinct characteristic as shown in Figure 3b. It can be observed that a higher transient that might reach up to 2.3 p.u., at the initial instant of the fault depending on the phase and this contribution shows a decaying behaviour can be observed. Unlike the one observed in the case of GFL converter, the transient observed from the GFM converter lasts longer as it may last for around eight cycles. This time-decaying characteristic is somehow emulating the SG behaviour. After that, and similar to the GFL case, the transient contribution is followed by the steady-state fixed value that is limited to the maximum overrating capability of the converter (i.e. 1.2 p.u.). It is worth noting that the phases experience different transient values due to the different inspection times of the fault at the voltage of each phase. Note that this sentence has been added to clarify this point.

In general, it can be observed that the SC current behaviour of the GFM converter is different from the one observed from GFL converters in terms of the transient behaviour and the time required to limit the current contribution. This might be due to the fast current controllers utilized in the GFL converters that activate the current limiting mode immediately after sensing the voltage dip event by injecting the additional reactive current with a minimum delay. On the other hand, as the GFM converters are controlled to mimic the SG behaviour, they inherently inject reactive current with no delays immediately after sensing the fault. However, this would limit the current but in a slower time when compared to the GFL case. In addition, the virtual impedance limiting strategy might lead to a decrease of the magnetic flux in the converter's transformer, which causes a DC offset in the magnetic flux, hence, a higher current that requires a longer time to decay. Of course, adopting such a strategy would necessitate the need for switches with higher overrating capability to be able to carry the current that appears before it is limited. In other words, as mentioned in Section 2, the damping and the current limiting procedure is based on the voltage drop through the virtual impedance in the event of SC faults. Hence, it may need a longer time to enter the current-limiting mode, as observed in Figure 3b.

4.2 | Voltage dip propagation under different penetration scenarios of GFL and GFM converters

To achieve the goal of this paper in examining the impact of GFM converters on the voltage dip propagation, the IEEE 9-bus test system [22] has been modelled in DIgSILENT PowerFactory where the studied scenarios are simulated. At first, the original system (base scenario of 0% penetration of RESs, that is, SGs only) has been considered and a three-phase bolted SC fault is created to test the voltage level during the fault at all buses other than the faulty bus (i.e. Bus 6 here). Then, the same process has been repeated considering three scenarios of converter-interfaced RESs represented by type-4 wind generators that utilize the GFL converter to examine the impact of the increased RESs' penetration on the voltage dip seen during the fault. Note that the scenarios have been selected based on the replacement of two out of three SGs connected originally in the test system. At first, SG3 of the minimum MVA is replaced to represent a low penetration scenario, then SG2 is replaced only keeping SG3 to represent a medium penetration scenario. At last, a high penetration scenario is created by considering the replacement of both SG2 and SG3 as shown in Figure 4. The formula indicated in (3) can be used to express the metric used to show the penetration level p, of RESs to the system's overall generation capacity.

$$p\% = \frac{Installed\ RESs\ (MVA)}{Total\ Installed\ Capacity\ (MVA)} \times 100\% \tag{3}$$

These scenarios are:

- **Scenario 1**: 22.5% penetration of RESs (SG3 is replaced by type-4 wind) (as shown in Figure 3).
- **Scenario 2**: 34.8% penetration of RESs (SG2 and SG3 are replaced by type-4 wind).
- **Scenario 3**: 57% penetration of RESs (SG2 and SG3 are replaced by type-4 wind).

Afterwards, the RESs based on GFL converters (type-4 wind generators) are displaced with GFM converters where the system is simulated again considering the same SC fault for both studied scenarios. This allows comparing the impact of the converter technology on the dynamic strength of the system represented by the voltage dip propagation through the network buses during faulty conditions. It is important to note that in each scenario, the total installed generation capacity stays the same. In other words, RESs installation capacity would be complemented by decommissioned SGs with the same capacity.

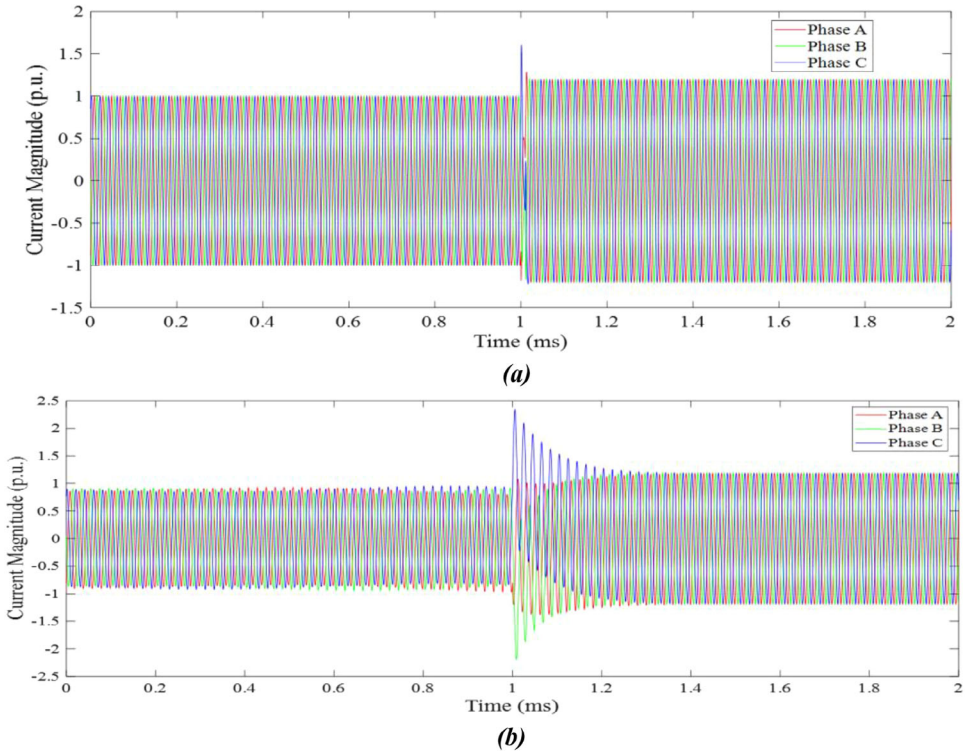

FIGURE 3 SC current contribution of converters (a) GFL, (b) GFM. GFL, grid-following; GFM, grid-forming; SC, SC, short circuit.

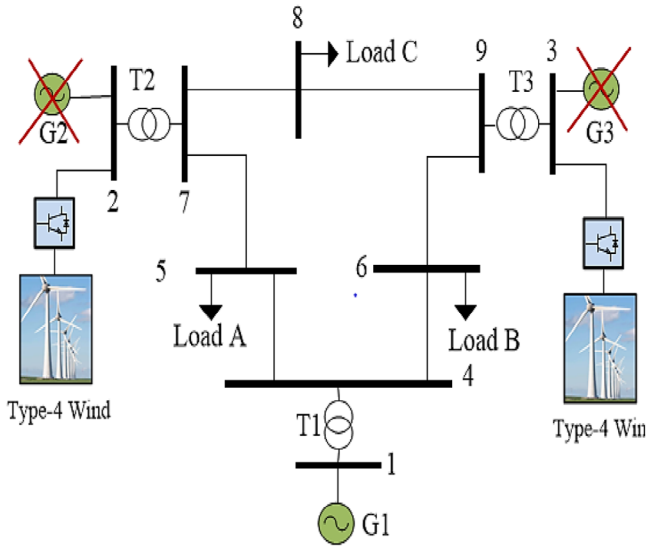

FIGURE 4 The adjusted IEEE 9-bus system with RESs (scenario 3). RES, renewable energy source.

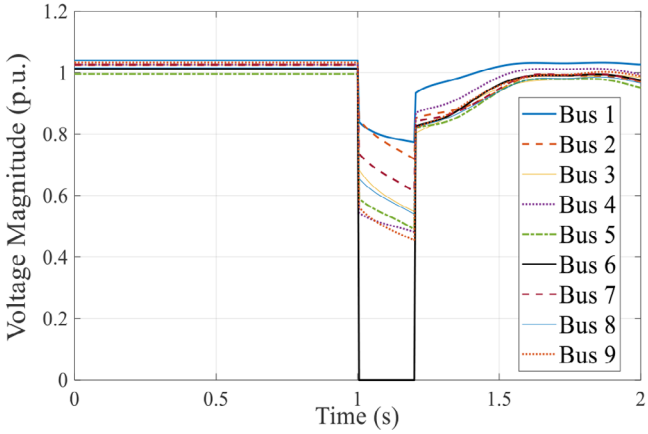

FIGURE 5 The voltage waveform at all buses (base scenario).

4.2.1 | Base scenario (SGs only)

As previously discussed, this scenario of SGs only is considered as a base scenario in which the voltage dip propagation due to a three-phase bolted SC fault is studied. Thus, it provides a preliminary insight on the system strength when considering SGs only. The SC fault is created at bus 6 where the voltage is dropped to almost zero during the fault. The voltage at all other buses is monitored and the during-fault voltage is observed to understand the voltage dip propagation through the network. Observe Figure 5, which shows the waveform of the voltage of the system buses before, during, and after the SC fault. Note that the SC fault is initiated after 1 s and lasts for 200 ms, where the SC fault is cleared at 1.2 s. The minimum voltage level at each bus has been obtained and represented in bars as shown in Figure 6.

It can be observed that the fault caused a very significant voltage dip at the faulty bus (i.e. bus 6) which shows a voltage of almost zero. The voltage dip has been propagated through the network with a serious impact that can be seen on the adjacent buses. For instance, buses 9, 4, and 5 have registered the lowest

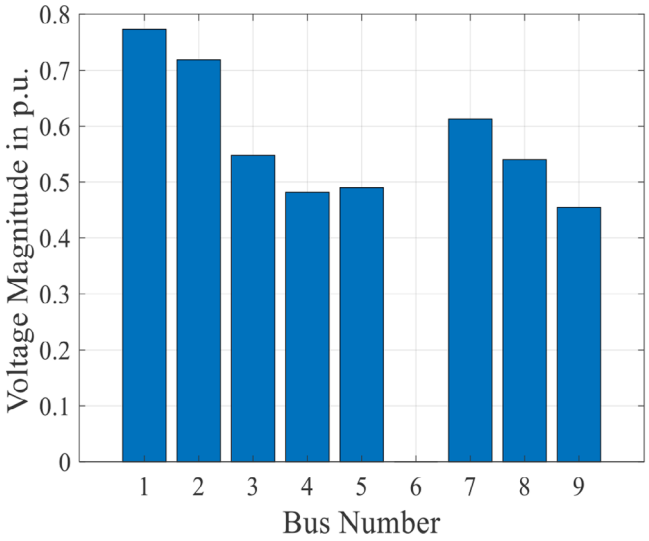

FIGURE 6 The minimum bus voltages during the fault (base scenario).

values of the voltage during the SC fault of 0.454, 0.481, and 0.489 p.u., respectively. On the other hand, those buses that are electrically far from the faulty bus have been less affected by the SC fault as their voltages have registered higher voltage levels.

Observe that bus 1 which is connected to the slack generator has the highest voltage during the fault as it has a stronger connection to the generation centre. Simultaneously, this bus shows a smoother voltage recovery after clearing the fault. Although other buses have witnessed severe voltage reduction during the fault, they all have achieved a voltage recovery and converged to the pre-fault steady-state voltage too. Hence, it can be concluded that the classical systems based on SGs only have decent system strength that allows them to recover their steady-state and operate stably after clearing the fault. In other words, dynamic voltage support provided by the SGs can help the system to recover. It is worth noting that an average of voltage dip considering all buses is around 0.513 p.u.

4.2.2 | RESs penetration Scenarios

Scenario 1: 22.5% RESs penetration level

In this scenario, both GFL- and GFM-based RESs are installed to replace the SG3. The SC fault has been initiated again at the same bus to investigate the voltage dip propagation at such a scenario.

GFL-based RESs. When integrated into the system, type-4 wind generators that are based on GFL converters have been utilized to form the wind farm connected at G3. The voltage dip propagation through the network is investigated by monitoring the voltage waveforms and the minimum voltage level during the fault at all system buses. The waveforms of the bus voltages are presented in Figure 7a. It can be observed that the voltage dip propagation is more severe than the previous level observed at the base scenario. In addition, the voltage during the fault has witnessed more distortion as voltage dip spikes have been

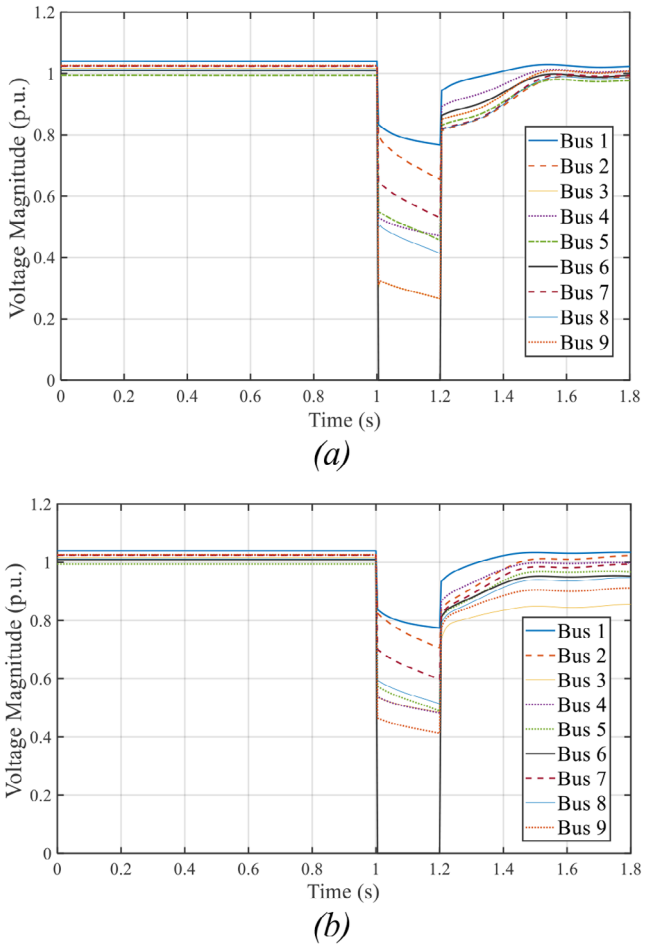

FIGURE 7 Voltage waveform at all buses (scenario 1): (a) GFL converters, (b) GFM converters. GFL, grid-following; GFM, grid-forming.

observed immediately after the fault. The minimum voltage dip observed considering GFL-based RESs (type-4 wind generators) is more severe at the adjacent buses of the faulty bus (i.e. bus 6). All the buses registered lower values than those obtained from the base scenario. For example, buses 9, 3, and 8 have registered the lower values of the voltage during the SC fault of 0.270, 0.266, and 0.41 p.u., respectively. It is worth pointing out that the average voltage dip observed on all buses is around 0.421 p.u., which is around 0.092 p.u. lower than the base scenario. It is also notable that bus 3, where the wind generator is installed, has witnessed the most reduction in the voltage level during the fault. For instance, it has reduced from 0.547 p.u down to around 0.266 p.u, which represents a reduction of 0.281 p.u.

GFM-based RESs. Considering the same scenario of 22.5% RESs penetration but with GFM converters, the voltage dip propagation through the network has been mitigated. Observe that not only the level of the voltage during the fault has become bigger and closer to the levels obtained from the base scenario, but also the waveforms have shown smother transient voltage too. Figure 7b shows the waveforms of the bus voltages during the fault when GFM converters are considered. Observe

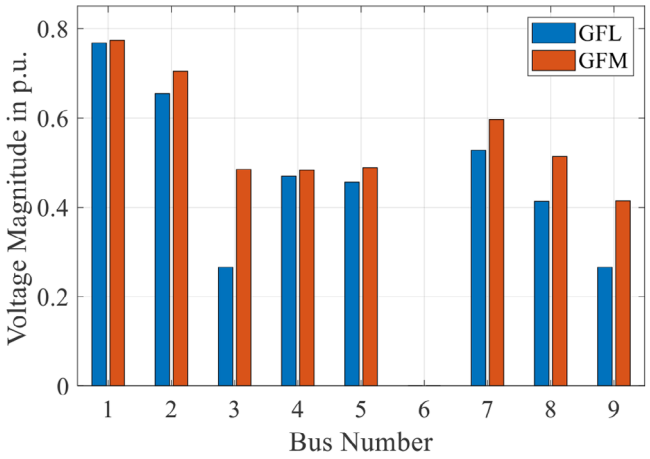

FIGURE 8 Minimum bus voltages during the fault (scenario 1).

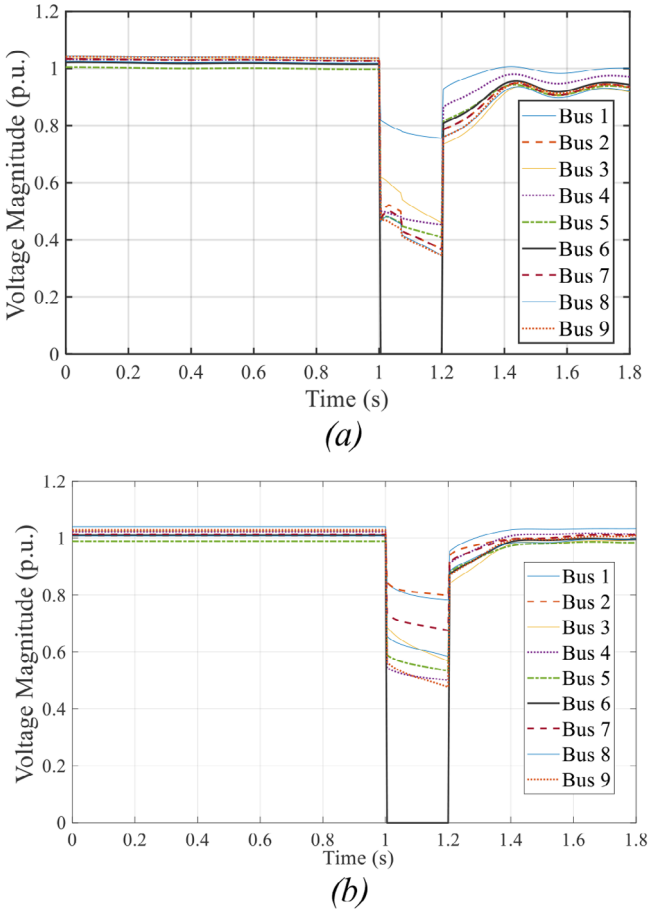

FIGURE 9 Voltage waveform at all buses (scenario 2): (a) GFL converters, (b) GFM converters. GFL, grid-following; GFM, grid-forming.

that although the level of the voltage dip is lower than the base scenario levels, these registered voltage dip levels have been mitigated and the response of the voltages is enhanced when compared to those of the GFL converter case. For instance, less distorted dynamic voltages with less spikes have been observed and the average voltage dip though the network buses has been mitigated from 0.421 p.u. at the GFL case up to 0.50 p.u. in the GFM case. More specifically, bus 3 voltage dip level, where the GFM converter is connected, has witnessed a considerable increment from 0.266 p.u. in the GFL case, up to 0.485 p.u in the GFM case. This represents a 0.219 p.u. However, this is still less than the base scenario level of 0.547 p.u. The comparison of both cases (GFL and GFM) at 22.5% penetration scenario is provided by Figure 8. It can be also observed that the closer the bus to the GFM converter, the more enhancement of the voltage dip level is observed as observed for buses 3 and 9. On the other hand, the response of the voltage recovery in the case of GFM converters has not shown mitigated behaviour at some buses as shown in Figure 7b.

Scenario 2: 34.8% RESs penetration level

In this scenario, both GFL- and GFM-based RESs are installed to replace SG2. The SC fault has been initiated again at the same bus to investigate the voltage dip propagation at such a scenario which represents a high penetration scenario of RESs.

GFL-based RESs. After getting integrated into the system, type-4 wind generators that are based on GFL converters have been utilized to form the wind farm connected at G2 to replace SG2. This RESs penetration forms 34.8% of the whole installed generation capacity in the system as per the metric in Equation (3). Like the previous scenarios, the voltage dip propagation through the network is investigated by monitoring the voltage waveforms and the minimum voltage level during the fault at all system buses. The waveforms of the bus voltages are presented in Figure 9a. It can be observed that the voltage dip propagation is more severe than the previous level observed at the those observed in scenario 1. However, there has been neither distortion nor any witnessed change in voltage during the fault. The minimum voltage dip observed concerning GFL-based RESs (type-4 wind generators) is more severe at the adjacent buses of the faulty bus (i.e. bus 6). All the buses registered lower values than those obtained from the ones observed at scenario 1. It is worth noting here that the most affected buses are not only those close to the faulty bus, but also the bus where the GFL-RES is located has shown almost the most severe reduced voltage during the fault. This is a crucial finding which proves that the GFL-based RESs fails to support the dynamic voltage as intended. For instance, bus 2 which is directly connected to the RESs at G2 has shown the minimum voltage during the fault with a value of 0.366 p.u, as shown in Figure 10. Compared to scenario 1, bus 2 voltage has reduced from 0.654 p.u down to 0.366 p.u, which represents a significant reduction of 0.288 p.u. Regardless of the existence of a transformer connecting bus 7 to the GFL-based RES installed at G2, the voltage level at bus 7 has also witnessed almost the same reduction and registered the same voltage level of 0.366 p.u. On the other hand, although bus 8 is a bit electrically far from the faulty bus, it has registered the most reduced voltage as it is close to the G2. However, although the voltage of bus 8 is limited to 0.345 p.u, in scenario 2, it has shown a decent improvement when compared to the previous minimum level of 0.266 p.u., which has been registered in scenario 1. Apar from bus 1, which is still connected to the SG1,

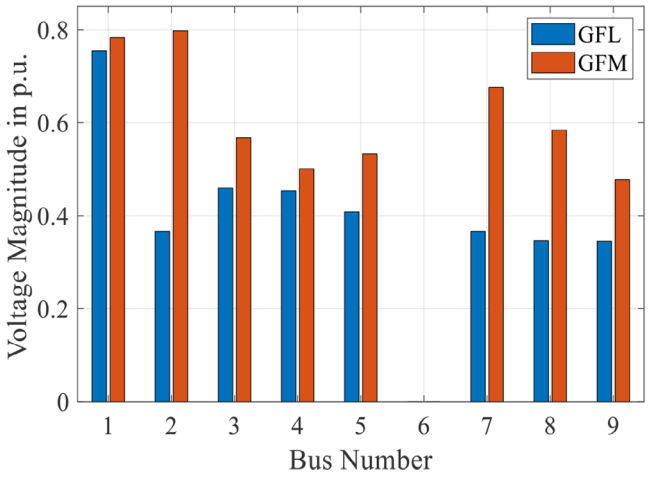

FIGURE 10 Minimum bus voltages during the fault (scenario 2).

all other buses have been negatively affected with an average voltage dip of 0.389 p.u, approximately.

GFM-based RESs. Considering the same scenario of 34.8% RESs penetration but with GFM converters, the voltage dip propagation through the network has been mitigated compared to the case of GFL converters as shown in Figure 9b. Observe that not only the level of the voltage during the fault has enhanced and is getting closer to the levels obtained from the base scenario, but also the waveforms have shown smother transient voltage too. The average voltage dip level observed in scenario 2 considering the GFM converters is around 0.546 p.u., which is better than the previously studied scenarios even more than the base scenario of SGs only, where an average of 0.513 p.u. has been observed. This indicates that the GFM converters are significantly positively reducing the impact of the voltage dip propagation, more specifically, at higher penetration scenarios such as 34.8% (e.g. scenario 2). Moreover, it can be observed that most of the buses have witnessed an improved dynamic voltage level during the SC fault regardless of the location. However, those buses directly connected to the GFM-based RESs are the most affected ones as shown in Figure 10. Note that although the GFM converter shows less fault current, the dynamic of the fault itself and the decaying characteristics are different. For instance, while the current contribution of the SGs is in the phase with the system, the fault current contribution of the converters is mostly reactive and independent of the phase of the system, which might interpret the better dynamic voltage support during the fault. More insight about the differences between the fault response of the SGs and converter-based RESs is provided in [9, 20, 23, 24]. Figure 5 shows how the slope of the voltage during the fault is sharper than the case of Figure 9 related to scenario 2.

Besides the positive impact observed at the voltage dip level when utilizing the GFM-based RESs, the voltage recovery in this scenario has been also improved as most of buses have successfully recovered and back to their pre-fault levels with almost 1 p.u. Observe Figure 9b which clearly shows how the voltage recovery after clearing the fault has converged to the pre-fault steady-state level at scenario 2 concerning GFM-based RESs. This in its turn indicates that the functionality of the GFM converters has performed well in supporting the grid voltage after clearing the fault.

Scenario 3: 57% RESs penetration level

In this scenario, both GFL- and GFM-based RESs are installed to replace the SG3 and SG2 to represent a 57% penetration of RESs. The SC fault has been initiated one more time at the same location (i.e. bus 6) to explore the voltage dip propagation at such scenario which represent a high penetration scenario of RESs.

GFL-based RESs. At first, type-4 wind generators that are based on GFL converters have been utilized to form the wind farm connected at G2 and G3 to replace SGs and SG3, respectively. This RESs penetration forms 57% of the whole installed generation capacity in the system considering the penetration metric expressed in Equation (3). Like the previous scenarios, the voltage dip propagation through the network is investigated by monitoring the voltage waveforms and the minimum voltage level during the fault at all system buses. The waveforms of the bus voltages are presented in Figure 11a. It can be observed that the voltage dip propagation is more severe than the previous level observed at the those observed at scenario 1. However, the voltage during the fault has not witnessed neither distortion nor. The minimum voltage dip observed concerning GFL-based RESs (type-4 wind generators) is more severe at the adjacent buses of the faulty bus (i.e. bus 6). All the buses registered lower values than those obtained from the ones observed at the previously studied scenarios. It is worth noting here that the most affected buses are not those close to the faulty bus; instead, the buses where the GFL-RESs are located have shown the most severe reduced voltage during the fault. This is a crucial finding which proves that the GFL-based RESs fail to support the dynamic voltage as intended. For instance, bus 3 which is directly connected to the RESs at G3 has shown the minimum voltage during the fault with a value of 0.122 p.u, as shown in Figure 12. Regardless of the existence of a transformer connecting bus 9 to the GFL-based RES installed at G3, the voltage level at bus 9 has also witnessed the same severe reduced voltage during the fault (i.e. 0.122 p.u.). Observe that this can be also applied to the voltage dip observed at buses 2 and 7 where the GFL-based RES (i.e., type-4 wind generator) is located to replace G2. Apar from bus 1, which is still connected to the SG1, all other buses have been severely affected with an average voltage dip of 0.27 p.u., approximately. It is worth pointing out that, unlike the case of scenario 2, the voltage during fault for the GFL case in scenario 3 has not experienced a distortion. This might be due to the sensitivity of the controller of GFL converter to the penetration level and the interaction and the phase jump between the reactive current injection from the converter itself and the other fault current component fed by the other SGs. For instance, observe that the most affected voltages (Buses 2, 7, 5, and 8) are electrically close to the location of the integrating converter (SG2) in scenario 2, where the fault

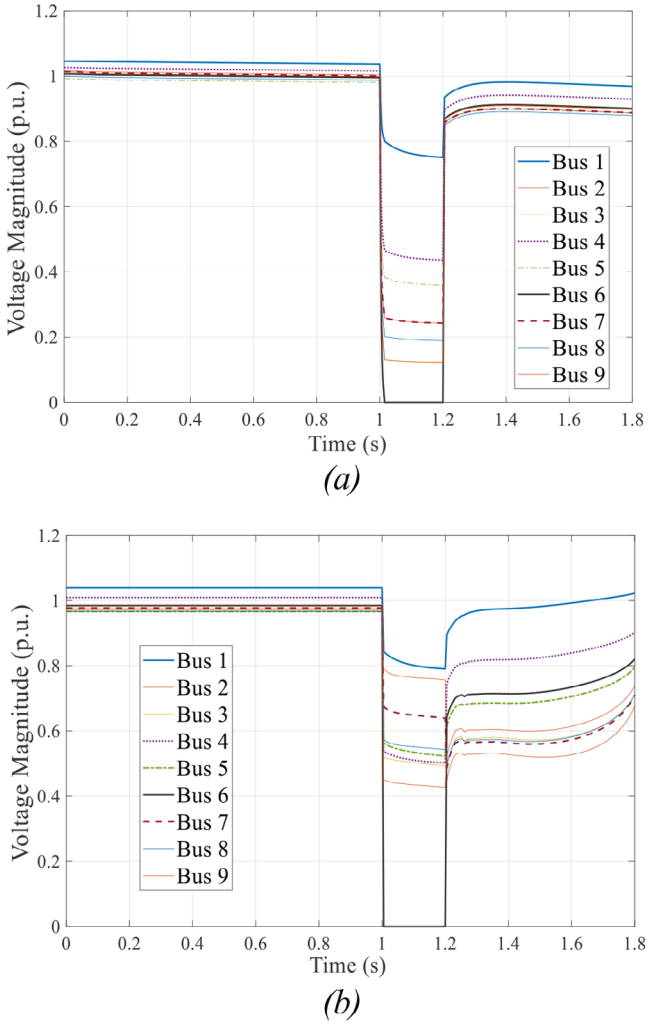

FIGURE 11 Voltage waveform at all buses (scenario 3): (a) GFL converters, (b) GFM converters. GFL, grid-following; GFM, grid-forming.

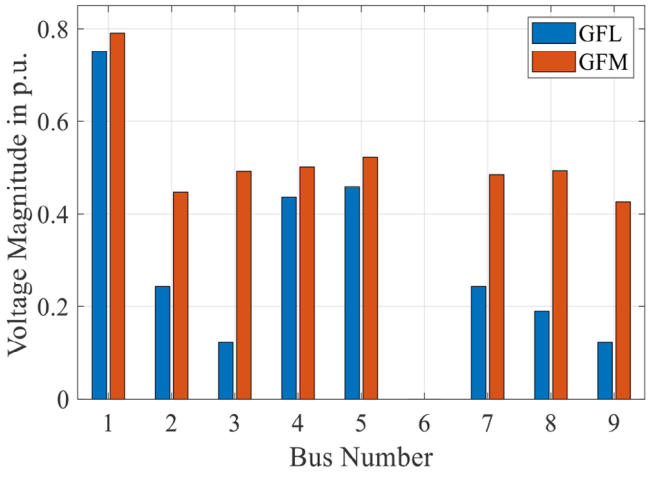

FIGURE 12 Minimum bus voltages during the fault (scenario 3).

current of the SGs is dominant. On the other hand, the reactive current injection from the converter is predominant in scenario three, where two converters are considered to replace SG2 and SG3 together.

GFM-based RESs. Considering the same scenario of 57% RESs penetration but with GFM converters, the voltage dip propagation through the network has been remarkably mitigated compared to the case of GFL converters as shown in Figure 11b. Observe that not only the level of the voltage during the fault has enhanced and is closer to the levels obtained from the base scenario, but also the waveforms have shown smother transient voltage too with no distortions. The average voltage dip level observed in scenario 3 considering the GFM converters is around 0.462 p.u, which is better than all other studied scenarios where RESs are considered. However, it is still less than the base scenario of SGs only, where an average of 0.513 p.u. has been observed. This indicates that the GFM converters are significantly positively reducing the impact of the voltage dip propagation, even at high penetration scenarios such as 57% (e.g. scenario 3). Moreover, it can be observed that most of the buses have witnessed an improved dynamic voltage level during the SC fault regardless of the location. However, those buses directly connected to the GFM-based RESs are the most affected ones as shown in Figure 12.

Despite the positive impact observed at the voltage dip level when utilizing the GFM-based RESs, the voltage recovery in the case of high RES's penetration (e.g. 56% penetration of scenario 2) has suffered from distortions and witnessed an oscillatory behaviour. Observe Figure 11b which clearly shows how the voltage recovery after clearing the fault has not converged to the pre-fault steady-state level at scenario 3 concerning GFM-based RESs. This in its turn indicates that the functionality of the GFM converters might not be adequate in terms of supporting the grid voltage after clearing the fault. Hence, they require more investigations and improvements to be able to cope with the potential increasing penetration of RESs, more specifically those scenarios of penetration levels that exceed 50%.

5 | CONCLUSION

This paper examines the effect of employing GFM converters for interfacing RESs on voltage dip propagation over networks in renewable energy-rich power systems. More specifically, those GFM converters that are based on droop control are utilized to mimic the behaviour of SGs. Using an IEEE 9-BUS test system modelled in DIgSILENT PowerFactory, the study of this research has considered several scenarios of converter-interfaced RESs equipped with traditional GFL and with GFM converters. At first, the SC current contribution of both types of converters (i.e. GFL and GFM) is investigated and compared for better understanding the dynamic voltage support performance during system faults like SC faults. Then, the voltage dip propagation into the network due to three-phase bolted SC faults has been analyzed considering classical systems based on

SGs only. After that, the impact of the increased penetration of converter-interfaced RESs on the voltage dip level during the faults has been examined considering both GFL and GFM converters technology.

The paper's findings conclude that the voltage dip propagation into the grid is significantly affected by the increased penetration of RESs. More specifically, the GFL-based RESs would severely reduce the dynamic voltage during the fault. Not only the voltage level during the fault might be affected, but also the distortion level and voltage recovery after clearing the fault would be negatively affected too. On the other hand, installing GFM converters has improved voltage behaviour by mitigating the voltage dip propagation through the network. The minimum level of the voltage and the distortion during the fault have been mitigated considerably. However, the voltage recovery after the fault clearing has shown a sensitivity to the penetration level of GFM converters. For instance, the voltage has been smoothly recovered at a low penetration level of GFM-based RESs, as observed in scenario1 and scenario 2. Conversely, the voltage recovery at higher penetration scenarios such as 57% penetration of GFM-based RESs has shown an oscillatory behaviour, and the voltage could not recover smoothly as observed at lower penetration scenarios.

Remarkably, the GFM converters have led to lower voltage dip propagation at medium penetration scenario like scenario 2 (i.e. 34.8% penetration) even better than the base scenario (SGs only). This might lead to the conclusion that the GFM converters have an excellent dynamic voltage support capability compared to SGs and GFL converters at some scenarios. However, this might not be valid at higher scenarios like 57%. In addition, they suffer when supporting the voltage recovery, specifically in high penetration scenarios exceeding 50%. It is noteworthy that further future investigations might be required to validate the applicability of GFM converters employing diverse current-limiting strategies. This is particularly important given the overrating capability of the converters, which may pose a challenge in implementing effective control strategies for applications such as voltage dip mitigation in renewable-rich power systems.

AUTHOR CONTRIBUTIONS

Rafat Aljarrah: Conceptualization; investigation; methodology; software; validation; visualization; writing—original draft. **Mazaher Karimi**: Methodology; project administration; supervision; validation; writing—review and editing. **Rasoul Azizipanah-Abarghooee**: Methodology; validation; visualization; writing—review and editing. **Qusay Salem**: Methodology; validation; visualization; writing—review and editing. **Sahban Alnaser**: Investigation; methodology; validation; visualization; writing—review & editing.

ACKNOWLEDGEMENTS

Part of this work was supported by the University of Vaasa through the Centralized Intelligent and Resilient Protection Schemes for Future Grids Applying-5G (CIRP-5G) Project with financial support provided by Business Finland under Grant 6937/31/2021. The authors would like to acknowledge the support from Princess Sumaya University for Technology.

CONFLICT OF INTEREST STATEMENT

The authors declare no conflict of interest.

DATA AVAILABILITY STATEMENT

No external data has been used for this research.

ORCID

Rafat Aljarrah https://orcid.org/0000-0003-2132-5333
Mazaher Karimi https://orcid.org/0000-0003-2145-4936

REFERENCES

1. Hartmann, B., Vokony, I., Táczi, I.: Effects of decreasing synchronous inertia on power system dynamics—Overview of recent experiences and marketisation of services. Int. Trans. Electr. Energy Syst. 29(12), e12128 (2019)
2. Aljarrah, R., et al.: Relationship between fault level and system strength in future renewable-rich power grids. Appl. Sci. 13(1), 142 (2023)
3. Gao, X., et al.: Stability analysis of grid-following and grid-forming converters based on state-space model. In: 2022 International Power Electronics Conference (IPEC-Himeji 2022-ECCE Asia), IEEE (2022)
4. Aljarrah, R., et al.: Monitoring of fault level in future grid scenarios with high penetration of power electronics-based renewable generation. IET Gener. Transm. Distrib. 15(2), 294–305 (2021)
5. Paspatis, A., et al.: Dynamic grid voltage support from distributed energy resources during short-circuits. In: 2017 52nd International Universities Power Engineering Conference (UPEC), IEEE (2017)
6. Lammert, G., et al.: Impact of fault ride-through and dynamic reactive power support of photovoltaic systems on short-term voltage stability. In: 2017 IEEE Manchester PowerTech, IEEE (2017)
7. Camacho, A., et al.: Active and reactive power strategies with peak current limitation for distributed generation inverters during unbalanced grid faults. IEEE Trans. Ind. Electron. 62(3), 1515–1525 (2014)
8. Khan, S.A., et al.: Grid-forming converters for stability issues in future power grids. Energies 15(14), 4937 (2022)
9. Aljarrah, R.R.: Assessment of Fault Level in Power Systems with High Penetration of Non-Synchronous Generation. The University of Manchester (United Kingdom) (2020)
10. Aljarrah, R., H. Marzooghi, V. Terzija: Mitigating the impact of fault level shortfall in future power systems with high penetration of converter-interfaced renewable energy sources. Int. J. Electr. Power Energy Syst. 149, 109058 (2023)
11. Bikdeli, E., et al.: State of the art of the techniques for grid forming inverters to solve the challenges of renewable rich power grids. Energies 15(5), 1879 (2022)
12. Rathnayake, D.B., et al.: Grid forming inverter modeling, control, and applications. IEEE Access 9, 114781–114807 (2021)
13. Pattabiraman, D., R. Lasseter, T. Jahns: Comparison of grid following and grid forming control for a high inverter penetration power system. In: 2018 IEEE Power & Energy Society General Meeting (PESGM), IEEE (2018)
14. Pattabiraman, D., R.H. Lasseter, T.M. Jahns: Short-term voltage stability of power systems with high inverter penetration under small disturbances. In: 2019 IEEE Power & Energy Society General Meeting (PESGM), IEEE (2019)
15. Sproul, S., et al.: System strength support using grid-forming energy storage to enable high penetrations of inverter-based resources to operate on weak networks. In: Cigre Paris Sessions 2022, CIGRE (2022)
16. Eberlein, S., Rudion, K.: Small-signal stability modelling, sensitivity analysis and optimization of droop controlled inverters in LV microgrids. Int. J. Electr. Power Energy Syst. 125, 106404 (2021)
17. Awal, M., et al.: Droop and oscillator based grid-forming converter controls: A comparative performance analysis. Front. Energy Res. 8, 168 (2020)

18. Wang, X., et al.: Virtual-impedance-based control for voltage-source and current-source converters. IEEE Trans. Power Electron. 30(12), 7019–7037 (2014)
19. PowerFactory: DIgSILENT Grid-Forming Converter Templates. In: Technical Reference. DIgSILENT GmbH (2021)
20. Aljarrah, R., et al.: Sensitivity analysis of transient short circuit current response to the penetration level of non-synchronous generation. Int. J. Electr. Power Energy Syst. 125, 106556 (2021)
21. Todorović, I., Grabić, S., Ivanović, Z.: Grid-connected converter active and reactive power production maximization with respect to current limitations during grid faults. Int. J. Electr. Power Energy Syst. 101, 311–322 (2018)
22. Anderson, P.M., A.A. Fouad: Power System Control and Stability. John Wiley & Sons (2008)
23. Tang, W., et al.: Short-circuit current of grid-connected voltage source converters: Multi-timescale analysis method. In: 2017 IEEE Power & Energy Society General Meeting, IEEE (2017)
24. Liu, C., Cai, X., Li, R., Yang, R.: Optimal short-circuit current control of the grid-forming converter during grid fault condition. IET Renew. Power Gener. 15(10), 2185–2194 (2021)

How to cite this article: Aljarrah, R., Karimi, M., Azizipanah-Abarghooee, R., Salem, Q., Alnaser, S.: Voltage dip propagation in renewable-rich power systems utilizing grid-forming converters. IET Renew. Power Gener. 1–11 (2024).
https://doi.org/10.1049/rpg2.12939